NANO LETTERS

LETTER

pubs.acs.org/NanoLett

Efficient and Directed Nano-LED Emission by a Complete Elimination of Transverse-Electric Guided Modes

Mei-Ling Kuo,[†] Yong-Sung Kim,[†] Mei-Li Hsieh,[*,‡,†] and Shawn-Yu Lin[*,†]

[†]The Future Chips Constellation and The Department of Physics, Applied Physics and Astronomy, Rensselaer Polytechnic Institute, Troy, New York 12180, United States

[‡]National Taiwan Normal University, Institute of Electro-Optical Science and Technology, National Taiwan Normal University, Taipei 116, Taiwan

ABSTRACT: A key to the success of solid-state lighting is an ultraefficient light extraction, ~90%. Recent advances in nanotechnology, particularly in creating nanorods, present an unprecedented opportunity to manipulate optical modes at nanometer scales. Here, we report an optically pumped nanorod light-emitting diode (LED) with an ultrahigh extraction efficiency of 79% at λ = 460 nm without the use of either a back reflector or thin film technology. We demonstrated experimentally three key mechanisms for achieving high efficiency: guided mode-reduction, embedded quantum wells, and ultraefficient light out-coupling by the fundamental HE_{11} mode. Furthermore, we show that size reduction at nanoscale represents a new degree-of-freedom for alternating and achieving a more directed LED emission.

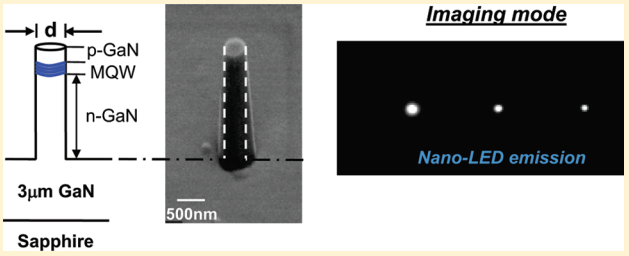

KEYWORDS: Light-emitting-diode, light extraction efficiency, optical guided modes, nanorod

GaN-based light-emitting diodes (LEDs) are an attractive light source for illumination purposes[1−3] due largely to their high efficiency and long lifetime. A compact, bright, and directed LED is also attractive for emerging biosensing and bioimaging applications.[4,5] One major factor that contributes to a highly efficient LED is the continuing improvement of internal quantum efficiency.[6,7] Another one is the improvement in extracting light that is otherwise trapped inside a high index GaN material.[8−10] The challenge associated with light extraction concerns the elimination of guided modes inside a LED.

Today, there are two types of surface-modified structures that are effective in extracting the trapped LED light. A thin-film, rough-surface LED with a back reflector can have a high extraction efficiency of ~80%.[11,12] The roughened surface is used to scatter light from the guided modes into the air. A thin-film, two-dimensional (2D) photonic-crystal LED can also give high extraction efficiency (~73%).[13] The photonic crystal is placed on top of quantum wells (QW) to diffract light into the air. Thin film LED geometry improves light extraction[13] by reducing the number of guided modes through size quantization along the growth direction (z direction). Unfortunately, to completely eliminate the guided modes, the film needs to be thin (50−100 nm), which is not practical for growth and current-spreading purposes. An alternative photonic-crystal approach is to etch 2D holes through the QWs.[14−17] Because the QW is inside a photonic crystal, light emission into guided modes may be eliminated due to a 2D photonic stop gap. An early calculation predicts an impressive, total light-extraction efficiency of >95% into the top and bottom surfaces.[14] However, the design has only been implemented in GaInAsP and with a moderate emission enhancement of 5 times.[15] Surface recombination and other scattering mechanisms may contribute to the limited success. The ultimate goal of light extraction at nearly 100% remains a challenge. Here, we adapt a different approach by decreasing the number of guided modes in the lateral direction along the QW plane (i.e., x and y direction) and by etching nanorods through the QWs. In the lateral size reduction process, guided modes are quantized and the number-of-modes can eventually approach a few and even one. Because the QW is part of a nanorod, an embedded emitter, light emission can be completely dictated by optical modes inside a nanorod.

In this paper, we demonstrated a large increase in light extraction due to guided-mode reduction, an embedded emitter design, and an ultraefficient light out-coupling by the fundamental HE_{11} mode. The complete mode elimination results in 79% light extraction efficiency without the use of either a back-reflector or a thin GaN film. We further illustrate that size reduction in the sub-λ scales can be used as a mean to modify a LED's radiation pattern.

The LED sample was grown on a sapphire substrate. The multiquantum wells consist of six periods of $In_{0.23}Ga_{0.77}N$/GaN and are sandwiched between a 125 nm p-type GaN and 4 μm n-type and undoped GaN layers. The nanorod LED was produced using a direct electron-beam-write method followed by

Received: September 14, 2010
Revised: November 16, 2010
Published: December 20, 2010

 © 2010 American Chemical Society

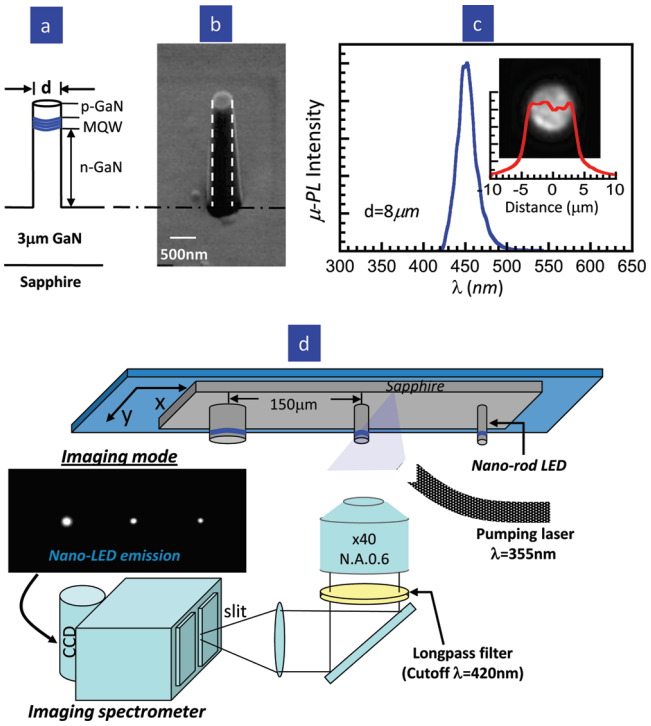

Figure 1. Scanning electron micrograph (SEM) image of a nanorod LED and the microphotoluminescence (μ-PL) setup. (a) A schematic of the nanorod LED layer structure, including the multiquantum well (MQW) layer of 100 nm. (b) A SEM image of a fabricated nanorod LED with a nominal rod diameter of d = 300 nm. (c) μ-PL spectrum of a nanorod LED with $d = 8\mu$m. Inset: a CCD scan image of the same nano-LED and its intensity profile (red curve) across the center of the rod. (d) A schematic of the μ-PL and imaging measurement setup.

metal deposition (nickel) and lift-off processes. The nanorod has a diameter ranging from d = 50 nm to 8 μm and an etch depth of ~1.4 μm. The detailed nanofabrication process is described elsewhere.[18] A schematic of the nanorod structure is shown in Figure 1a. The blue line indicates the QW regime, which is part of the etched cylindrical nanorod. A scanning electron micrograph (SEM) of a fabricated nanorod is shown in Figure 1b. The rod has a diameter of d = 300 nm, a smooth sidewall, and a slight tapering angle of ~10°.

The nanorod LED was studied using a microphotoluminescence (μ-PL) setup with a nanoimaging capability.[19] The setup consists of an inverted microscope and is shown schematically in Figure 1d. To achieve optical pumping, an Nd: YAG 355 nm laser is coupled to a 50 μm diameter fiber and is placed a few micrometers away from the nano-LED. To ensure an identical optical excitation, the fiber is kept fixed while a series of nano-LEDs are mounted on a moving stage. The luminescence signal was collected by a 40× objective, passed through a λ = 420 nm long pass filter, and fed into a spectrometer and a charge-coupled device (CCD) camera. Our setup is capable of studying (1) an LED emission spectrum, (2) an LED emission image, and (3) a CCD scan intensity profile. As an illustration, we show, in Figure 1c, a typical testing result of a large LED with $d = 8\ \mu$m. In the spectroscopic mode, the μ-PL spectrum shows a peak emission at λ = 460 μm. In the image mode, the recorded LED emission image is shown in the inset. The intensity profile (the red curve) across the sample displays a slightly irregular intensity across the top surface, indicating multimode contribution from the LED emission.[13]

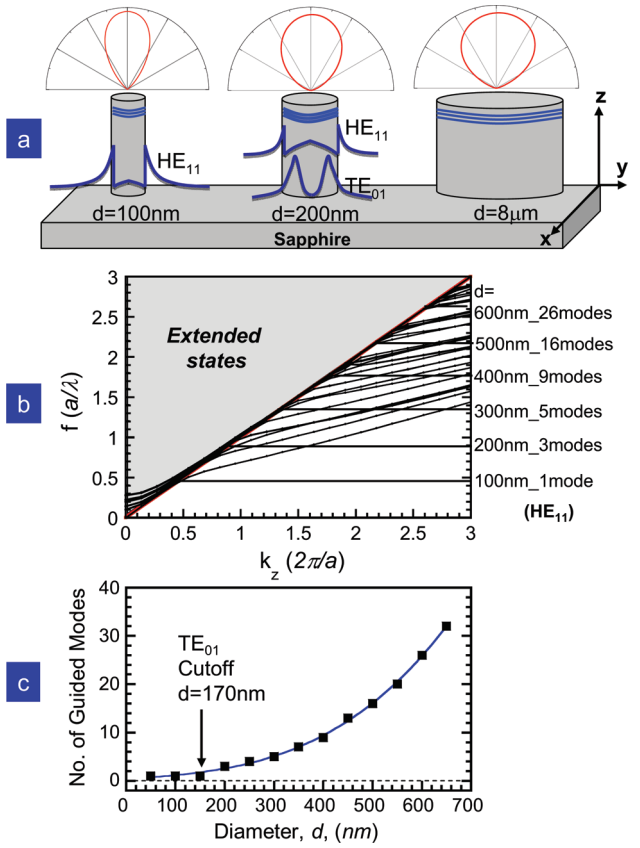

Figure 2. Modal and dispersion properties of a nanorod LED. (a) A schematic of the nanorod LED with different radiation patterns (red curves) and modal profiles (blue curves) for the fundamental HE_{11} and TE_{01} modes. (b) The frequency (f)−wavevector (k_z) diagram for cylindrical nanorod LEDs. The horizontal lines indicate the corresponding rod diameter and the number of guided modes inside the rod. (c) A summary of the number of guided modes inside the cylindrical rod as a function of the rod diameter.

To gain insight into light emission from relatively small nano-LEDs (d = 50−400 nm), we carry out modal and frequency-dispersion[20] calculations. The guided modes inside a cylindrical rod are solved analytically.[21] In Figure 2a, a schematic of the fundamental HE_{11} mode (blue curve) of the d = 100 nm nanorod and the first two modes of the d = 200 nm nanorod are shown. The lateral size reduction not only reduces the guided mode but also influences the radiation pattern of an LED. As "d" is reduced to 100−200 nm, the radiation pattern shows a significant deviation from a typical strong side-emission pattern of a planar LED and becomes much more directional. In Figure 2b, we show the frequency dispersion relationship, f vs k_z, of the nanorod. Here, the frequency f (a/λ) and k_z ($2\pi/a$) are both expressed in a normalized unit. The red line is the light line that separates the guided modes from the extended states (the gray region). While there are 26 guided modes for the d = 600 nm nanorod, the number-of-modes is significantly reduced to three and one for the d = 200 nm and 100 nm nanorod, respectively. The number of guided mode is summarized in Figure 2c as a function of d. The data show that the number-of-modes has a strong dependence on d and approaches 1 for d < 170 nm, i.e., the cutoff for the transverse electric (TE) mode. This represents a nanosize regime where emitted light from the QWs has the highest probability to escape into the air.

dx.doi.org/10.1021/nl103243n |Nano Lett. 2011, 11, 476–481

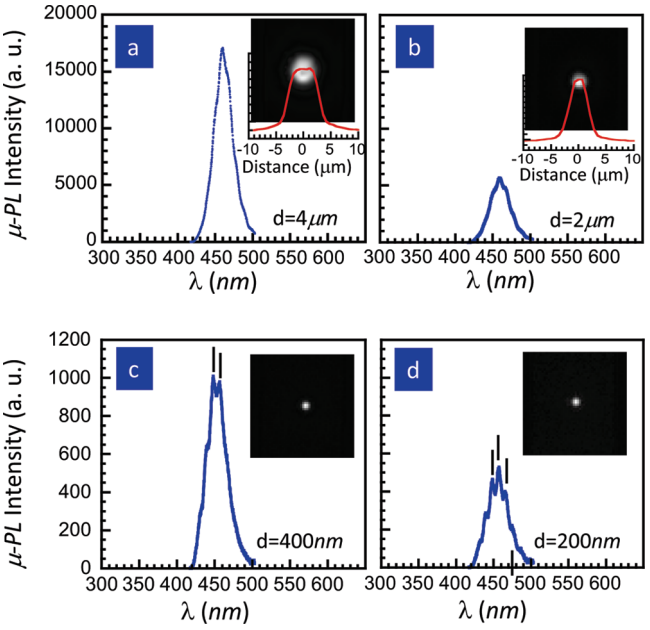

Figure 3. Microphotoluminescence (μ-PL) spectra and images from four nanorod LED devices. (a, b) μ-PL intensity spectra of nano-LEDs with a relatively large diameter, d = 4 and 2 μm, respectively. The peak emission wavelength is $\lambda \sim 455$ nm. Inset: the CCD image of nanorod LED with intensity profile. (c, d) μ-PL intensity spectra of nanorod LEDs with diameter, d = 400 and 200 nm, respectively. Inset: the CCD image of the nanorod LED.

In Figure 3, we show typical emission spectra of our nano-LEDs for four different rod diameters, d = 4 μm, 2 μm, 400 nm, and 200 nm. To obtain reliable emission data, we must be sure to excite one nano-LED at a time. This is achieved by making the spacing between adjacent nano-LEDs sufficiently wide (150 μm). We must also examine the image of a nano-LED emission for any unwanted background contribution. In the inset of Figure 3a, the CCD image shows an excellent image contrast with a bright, round spot and a dark background. The intensity line scan across the center of the rod (the red line) confirms that the emission is from the d = 4 μm nano-LED. The μ-PL data exhibit a peak at $\lambda \sim 460$ nm and an un-normalized intensity of 17000. The data for a d = 2 μm nano-LED are shown in Figure 3b. Again, the CCD image shows a bright spot and the line scan confirms that the emission is from the d = 2 μm nano-LED. The μ-PL shows a single peak at $\lambda \sim 460$ nm and a weaker intensity of 5700, a roughly 3-fold reduction in μ-PL intensity. It is noted that as d is decreased from 4 to 2 μm, the LED emission area is decreased by a factor of 4 and so should the μ-PL intensity. This comparison of μ-PL intensity to the LED's emitting area indicates that as d is decreased, nano-LED emission per area may be enhanced.

Next, we reduce the nanorod size to the sub-λ regime. In panels c and d of Figure 3, we show data taken from nano-LEDs with d = 400 and 200 nm, respectively. For such tiny nanoemitters, their respective CCD images are still bright and with little background noise. There is no line scan due to the finite pixel number of the emitter region. For the d = 400 nm nano-LED, its μ-PL spectrum shows a slight doublet with an intensity of 1000. For the d = 200 nm nano-LED, the μ-PL spectrum shows four weak peaks with an intensity of 540. The appearance of multiple emission peaks in μ-PL has been observed in other nanorod LED structures.[22,23] We note again that by reducing the rod size by a factor of 10, i.e., d = 2 μm to 200 nm, the nominal emitting area is reduced by a factor of 100 and yet the μ-PL intensity is reduced only by 11 times. Clearly, there exists a large enhancement of μ-PL intensity per emitting area as d is reduced to d = 200 nm. This observation confirms the prediction of Figure 2c, namely, as d is decreased, the number-of-guided modes is decreased and the extracting efficiency is increased accordingly. In theory, size quantization and mode reduction in waveguide geometry have been known for years. However, these data experimentally demonstrate, for the first time, a clear and unambiguous extraction enhancement of an order-of-magnitude.

In the following, we show results of a systematic study of μ-PL intensity as a function of rod diameter, from d = 8 μm to d = 50 nm. To obtain a statistical average, we measured four sets of nominally the same nano-LED. To obtain the total μ-PL intensity, the spectrum is integrated over λ = 430−510 nm. In Figure 4a, we plot the integrated intensity as a function d in a log−log scale for over 4 orders of magnitude. The open dots of each color represent the integrated intensity of one set of nano-LED and the black squares are the average value. The data are normalized to that obtained for d = 8 μm (the reference LED) and the dashed line indicates a "d^2-dependence", expected for a linear scaling of emission intensity vs emitting area. For d = 4−8 μm, the intensity follows closely the "d^2 dependence" well (as expected for a planar LED). For d = 100 nm to 1 μm, the intensity exhibits a significant deviation from the "d^2 dependence". For instance, at d = 200 nm, the integrated μ-PL intensity is about 20 times higher than that expected from a simple area-scaling behavior. For d < 80 nm, the integrated μ-PL intensity drops more severely as d is decreased. The observation of over an order-of-magnitude deviation from the expected d^2 dependence is striking and calls for a more detail analysis.

In our setup, the incident flux of the excitation laser is kept the same for all nano-LEDs and the μ-PL intensity is given by[3,6,11,13] μ-PL Intensity $\propto \eta_{\text{internal}} \times$ (emitting area) $\times C_{\text{ex}}$. If we have an accurate account of the emitting area and the internal quantum efficiency (η_{internal}), the extraction efficiency (C_{ex}) can be determined. First, we show that η_{internal} of our nano-LED is not affected significantly by the nanofabrication and etching process. To determine η_{internal}, we perform temperature-dependent PL measurement of our nano-LED. The nano-LEDs are arranged in a 2 × 2 mm^2 array for ease of optical testing at cryogenic temperatures, T=4−300 K. From this temperature-dependent measurement, η_{internal} of our nano-LED is determined and plotted in Figure 4c. The data show a slight variation of η_{internal} as a function of d, but with an average value of $\eta_{\text{internal}} = 40 \pm 5\%$ for d = 50 nm to 8 μm. These data show that the etching process does not have a significant impact on internal quantum efficiency[24] of our nano-LEDs. Second, to better define the emitting area, we take into account the slightly tapered nanorod geometry with a $\theta \sim 10^\circ$ tapering angle as shown in Figure 1b. This geometrical shape effectively increases the emitting area due to an additional top emission from the slightly tilted sidewall near the MQW regime. From the image in Figure 1b, the additional emitting area is non-negligible for d < 300 nm and needs to be included to avoid an overestimate of the μ-PL intensity per area. Accordingly, we define the effective emitting area as

$$A^{\text{eff}} = \pi\left[\left(\frac{d}{2}\right)+\frac{1}{2}(\Delta z \tan 10^0)\right]^2$$

The second term accounts for the additional area and the Δz (=100 nm) is the MQW thickness. Third, as d is varied, incident

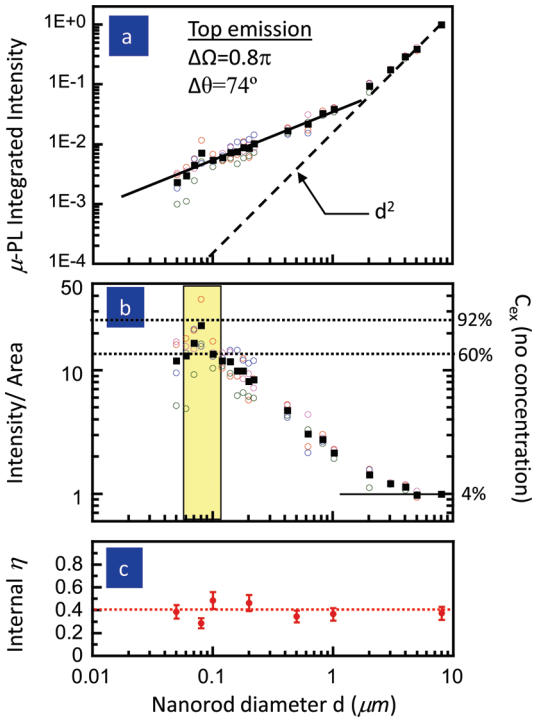

Figure 4. The rod diameter dependence of integrated μ-PL intensity, intensity/effective area, and the internal quantum efficiency. (a) Integrated intensity plot as a function of rod diameter d (μm). Four complete sets of nanorod LEDs with d = 8 μm to d = 50 nm were measured. Open dots of each color represent the intensity of one full set of LEDs. Black square dots represent the average of four sets measurement. The luminescence was from the top emission with a collection angle of $\Delta\Omega = 0.8\pi$. The dash line shows a "d^2 dependence", and solid black lines are guides to the eye. (b) The integrated intensity per effective emitting area as a function of d. The data are normalized to that obtained from the d = 8 μm LED, which one may be considered as a planar LED with a theoretical extraction efficiency of 4 ± 0.5% (corresponding to the right axis). (c) The internal efficiency as a function of nanorod diameter d. Red dash line is a guide to the eyes.

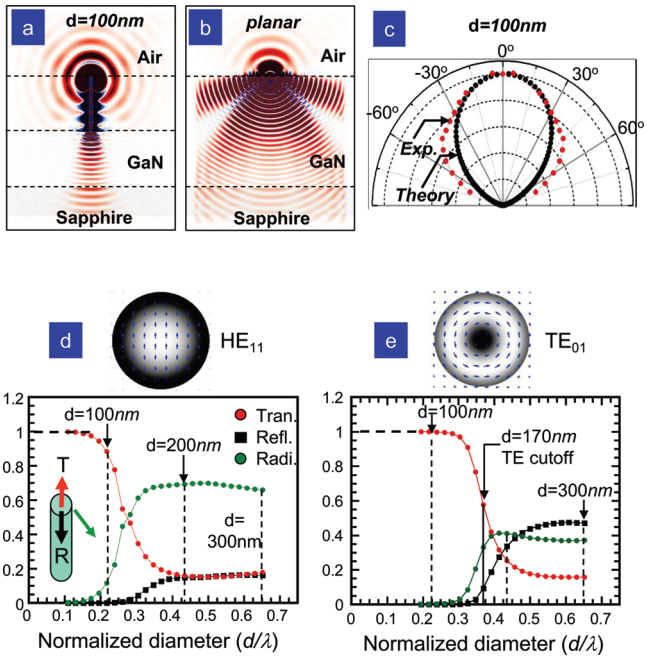

Figure 5. Guided mode properties of a nanorod LED and its far-field radiation pattern. (a) Results of a theoretical computation of the electric field intensity profile of a d = 100 nm nanorod LED. (b) Results of a theoretical computation of the electric field intensity profile of a planar LED. (c) An angular emission plot of a d = 100 nm nanorod LED obtained from an experimental (red dots) and a theoretical calculation (black dots). (d, e) Results of calculation of transmittance T (red dot), reflectance R (black square), and radiation amplitude (green dot) for fundamental HE_{11} and TE_{01} guided mode, respectively. The rod diameter is expressed in a normalized unit (δ/λ).

light may be reflected and absorbed differently. It is not easy to measure reflectivity of a nanorod as it is less than 1 λ. However, a previous measurement of array of nanorod shows a reflectivity of 30 ± 7% and is close to the value of a planar LED.[16] Our finite-different-time domain calculation of normal incident reflectance off the top surface of a single nanorod also indicates that nanorod reflectivity is close to the reflectivity of a planar GaN structure, 18.4%.

Using this effective light-emitting area, we plot the intensity/effective area as a function d in a logarithmic scale in Figure 4b. The open dots represent data taken from an individual set of nano-LEDs and the square dots are the average value. For ease of comparison, we set the intensity/area value to be 1 for the reference sample (d = 8 μm). In other words, this is the extraction value for a large-area, planar LED and should correspond to C_{ex}^{planar} = 4 ± 0.5% per surface for a $\Delta\Omega = 2\pi$ collecting solid angle.[3,25] In the large sample regime and for nano-LEDs with d = 4 and 8 μm, we see that the intensity/area magnitudes are the same and equal to 1. As d is decreased from 2 μm to 100 nm, the intensity/area is increased monotonically. In the small diameter regime with d = 60−120 nm, it reaches a large value of 14−23 (the two horizontal dashed lines) for a $\Delta\Omega = 0.8\pi$ collecting solid angle. These data suggest that our nano-LEDs should have a large extraction efficiency of C_{ex} = 60−92%, provided that the emitted light is not preferentially concentrated into a small angular range.

The influence of lateral size reduction on the angular distribution of a nano-LED emission is examined next. In Figure 5a, we show results of a FDTD field profile calculation of a nanorod with d = 100 nm or $d/\lambda \cong 0.20$. Inside the nanorod, electromagnetic wave (EM) propagates along the z direction into the substrate with a well-defined phase front. The top emission into the air also shows a more collimated propagation along the z direction. To confirm this prediction, we measure the radiation pattern of a nano-LED with d = 100 nm. Due to instrumentation limitation, the angular-dependent measurement is performed on a square array of nano-LED samples with a lattice constant of 400 nm and an array size of 2 × 2 mm^2. In Figure 5c, we show the measured (red dots) and the computational (black dots) results. The radiation does not follow either a strong side emission pattern of a planar LED or the Lambertian pattern. Instead, it is more directional with a half-power point at $\theta = 35°$. Taking this experimentally observed angular concentration effect into account, we find that the maximum extraction efficiency at $d \cong$ 100 nm is reduced from C_{ex} = 92% to C_{ex} = 79%. We may conclude that a nano-LED offers not only a new way to enhance light extraction but also a new degree-of-freedom to tailor LED's radiation pattern.

We note that for a planar LED the maximum extraction efficiency can only be C_{ex} = 50% from the top surface. Our data have an apparent violation of this upper limit. However, we note

dx.doi.org/10.1021/nl103243n |Nano Lett. 2011, 11, 476–481

from Figure 5a that the EM field intensity exhibits a stronger forward emission. For comparison purposes, the intensity profile for a planar LED is shown in Figure 5b. It shows a significantly stronger backward emission than forward emission. The preferred forward light propagation for the d = 100 nm nano-LED is one of the key factors for the observed, large C_{ex} = 79%. We further note that, even at d = 100 nm, there is one HE_{11} guided mode left (as shown in Figure 2b) to trap light inside the GaN sample. It is important to address the issue of light output coupling of the lowest guided mode for small nano-LEDs of 50 nm < d < 300 nm.

The unusually high extraction efficiency of our nano-LED for $d \leq 120$ nm may be understood by examining optical scattering properties of guided modes under sub-λ confinement. A full-vector Maxwell equation solver, the so-called, cavity modeling framework (CAMFR), is used to calculate the transmission, reflection, and radiation loss of our cylindrical, nanorod LED. Briefly, it is based on a frequency-domain Eigen mode expansion method. We have also implemented a supercell approach in cylindrical coordinates and perfectly-matched-layer boundary condition to avoid parasitic reflections.[26] In Figure 5d, we show transmittance, reflectance, and radiation amplitude vs the normalized diameter, (d/λ) computed for the fundamental HE_{11} mode. For $d/\lambda \geq 0.5$, the transmittance is low (~0.15), the reflectance is low (~0.15), and the radiation loss is high (~0.70). This is the large nanorod regime where light cannot be efficiently coupled to the air. However, for $d/\lambda \geq 0.22$, the reflectance is close to zero, the radiation loss is low and the transmittance is high (>0.85). A computed HE_{11} mode profile with E-field lines is also shown. This is the small nanorod regime where light in the HE_{11} mode can be easily out-coupled into the air. For our nano-LED, it emits at λ = 460 nm and the condition is satisfied for $d \leq 100$ nm. An earlier calculation for a quantum dot emitter shows a similar optical scattering property.[27,28] This unique optical property for nanoscale rod holds true for higher order modes as well. In Figure 5e, we show results calculated for the lowest order TE_{01} mode. The data show a similar trend as that for the fundamental HE_{11} mode. In this case, for $d/\lambda \geq 0.30$, the reflectance is close to zero and the transmittance is near unity. From this analysis, we may conclude that one of the key factors for achieving high extraction efficiency is an ultraefficient light out coupling of HE_{11} and TE_{01} modes. It is in this sub-λ regime, e.g., $d/\lambda \geq 0.20$, where the challenge of light trapping may be completely resolved.

Finally, it is noted that modal profile of a nanorod can extend outside of its structure. Overlap of the mode and the active quantum well of an LED might become an issue. We computed the fractional power inside the nanorod for cylindrical waveguide modes[29] and found that good overlap exists for d > 100 nm. Therefore, the optimum nanorod diameter is 100 nm < d < 200 nm, where there is a relatively strong overlap of the mode and the active medium and also a high transmittance (Figure 5d and Figure 5e) for light extraction.

In summary, we demonstrate that it is possible to completely eliminate TE guided modes inside a nanorod LED and accomplish an extraction efficiency of 79% from the top surface without the use of a back-reflector or a thin film. The keys to this success are to place the quantum wells inside the nano-LED and to reduce the rod diameter to a sub-λ confinement regime ($d/\lambda \leq 0.22$). We further illustrate new ways to control the radiation pattern using a nano-LED.

AUTHOR INFORMATION

Corresponding Author

*E-mail: mlh@ntnu.edu.tw (M-L.H.) or sylin@rpi.edu (S-Y.L.).

ACKNOWLEDGMENT

S.Y.L. gratefully acknowledges partial financial support from NSF under award No. EEC-0812056. We acknowledge Dr. S. K. Eah for his help with the imaging spectrometer and Zu-Po Yang with the direct electron beam write of nano-LED structures.

REFERENCES

(1) Walterett, P.; Brandt, O.; Trampert, A.; Grahn, H. T.; Menniger, J.; Ramsteiner, M.; Reiche, M.; Ploog, K. H. Nitride semiconductors free of electrostatic fields for efficient white light-emitting diodes. *Nature* **2000,** *406*, 865.

(2) Ponce, F. A.; Bour, D. P. Nitride-based semiconductors for blue and green light-emitting devices. *Nature* **1997,** 386.

(3) Phillips, J. M.; Coltrin, M. E.; Crawford, M. H.; Fischer, A. J.; Krames, M. R.; Mueller-Mach, R.; Mueller, G. O.; Ohno, Y.; Rohwer, L. E. S.; Simmons, J. A.; Tsao, J. Y. Research challenges to ultra-efficient inorganic solid-state lighting. *Laser Photonics Rev.* **2007,** *1* (No. 4), 307–333.

(4) Adato, R.; Yanik, A. A.; Amsden, J. J.; Kaplan, D. L.; Omenetto, F. G.; Hong, M. K.; Erramilli, S.; Altug, H. Ultra-sensitive vibrational spectroscopy of protein monolayers with plasmonic nanoantenna arrays. *Proc. Natl. Acad. Sci. U.S.A.* **2009,** *206* (no 46), 19227–19232.

(5) Cole, R. W.; Turner, J. N. Light-emitting diodes are better illumination sources for biological microscopy than conventional source. *Microsc. Microanal.* **2008,** *14* (03), 243.

(6) Watanabe, S.; Yamada, N.; Nagashima, M.; Ueki, Y.; Sasaki, C.; Yamada, Y.; Taguchi, T.; Tadatomo, K.; Okagawa, H.; Kudo, H. Internal quantum efficiency of highly-efficient $In_xGa_{1-x}N$-based near-ultraviolet light-emitting diodes. *Appl. Phys. Lett.* **2003,** *83* (24), 4906.

(7) Cao, X. A.; LeBoeuf, S. F.; D'Evelyn, M. P.; Arthur, S. D.; Kretchmer, J.; Yan, C. H.; Yang, Z. H. Blue and near-ultraviolet light-emitting diodes on free-standing GaN substrates. *Appl. Phys. Lett.* **2004,** *84* (21), 4313.

(8) Schnitzer, I.; Yablonovitch, E.; Caneu, C.; gmitter, T. J. Ultrahigh spontaneous emission quantum efficiency, 99.7% internally and 72% externally, from AlGaAs/GaAs/AlGaAs double heterostructures. *Appl. Phys. Lett.* **1993,** *62* (2), 131.

(9) Wu, M.-L.; Lee, Y. C.; Lee, P. S.; Kuo, C. H.; Chang, J. Y. III-Nitride-based microarray light-emitting Diodes with enhanced light extraction efficiency. *Jpn. J. Appl. Phys.* **2008,** *47* (8), 6757.

(10) Fujii, T.; Gao, Y.; Sharma, R.; Hu, E. L.; DenBaars, S. P.; Nakamura, S. Increase in the extraction efficiency of GaN-based light-emitting diodes via surface roughening. *Appl. Phys. Lett.* **2004,** *84* (6), 855.

(11) Krames, M. R.; Shchekin, O. B.; Muller-Mach, R.; Muller, G. O.; Zhou, L.; Harbers, G.; Craford, M. G. Status and Future of high Power Light emitting diodes for solid state lighting. *J. Disp. Technol.* **2007,** *3* (2), 160.

(12) Shchekin, O. B.; Epler, J. E.; Trottier, T. A.; Margalith, T.; Steigerwald, D. A.; Holcomb, M. O.; Martin, P. S.; Krames, M. R. High performance thin-flim flip chip InGaN-GaN light-emitting diodes. *Appl. Phys. Lett.* **2006,** *89*, No. 071109.

(13) Wierer, J. J.; David, A.; Megens, M. M. III-nitride photonic crystal light-emitting diodes with high extraction efficiency. *Nat. Photonics* **2009,** *3*, 163.

(14) Fan, S.; Villeneuve, P. R.; Joannopoulos, J. D.; Schubert, E. F. High extraction efficiency of spontaneous emission from slabs of photonic crystal. *Phys. Rev. Lett.* **1997,** *78* (17), 3294.

(15) Fujita, M.; Takahashi, S.; Tanaka, Y.; Asano, T.; Noda, S. Simultaneous inhibition and redistribution of spontaneous light emission in photonic crystals. *Science* **2005,** *308*, 1296.

(16) Kuo, M. L.; Lee, Y. J.; Shen, T. C.; Lin, S. Y. Large enhancement of light-extraction efficiency from optically pumped nanorod light-emitting diodes. *Opt. Lett.* **2009,** *34* (13), 2078.

(17) *Basic research needs for solid-state lighting* Report of the basic energy science workshop on solid-state lighting, May 22−24, 2006; p 133

(18) Huang, H. W.; Kao, C. C.; Hsueh, T. H.; Yu, C. C.; Lin, C. F.; Chu, J. T.; Kuo, H. C.; Wang, S. C. Fabrication of GaN-based nanorod light emitting diodes using self-assemble nickel nano-mask and inductively coupled plasma reactive ion etching. *Mater. Sci. Eng., B* **2004,** *113*, 125.

(19) The image spectrometer combines with Nikon inverted research microscopy (ECLIPSE TE2000) and CCD camera (PI-Max Princeton Instrument).

(20) Johnson, S. G.; Joannopoulos., J. D. Block-iterative frequency-domain methods for Maxwell's equations in a planewave basis. *Opt. Express* **2001,** *8* (No. 3), 173–190.

(21) Yariv, A. *Optical Electronics in Modern Communications*, 5th ed.; Oxford University Press: New York, 1997; Chapter 3.

(22) Hsieh, M. Y.; Wang, C. Y.; Chen, L. Y.; Ke, M. Y.; huang, J. J. InGaN-GaN nanorod light emitting arrays fabricated by silica nano-masks. *IEEE J. Quantum Electron.* **2008,** *44* (5), 468.

(23) Chang, Y. H.; Hsueh, T. H.; Lai, F. I.; Chang, C. W.; Yu, C. C.; Huang, H. W.; Lin, C. F.; Kuo, H. C.; Wang, S. C. Fabrication and microphotoluminescence investigation of Mg-Doped gallium nitride nanorods. *Jpn. J. Appl. Phys.* **2005,** *44* (4B), 2657.

(24) Chen, H. S.; Yeh, D. M.; Lu, Y. C.; Chen, C. Y.; Huang, C. F.; Tang, T. Y.; Yang, C. C.; Wu, C. S.; Chen, C. D. Strain relaxation and quantum confinement in InGaN-GaN nanoposts. *Nanotechnology* **2006,** *17*, 1454.

(25) Boroditsky, M.; Krauss, T. F.; Coccioli, R.; Vrijen, R.; Bhat, R.; Yablonovitch, E. light extraction from optically pumped light-emitting diode by thin-slab photonic crystals. *Appl. Phys. Lett.* **1999,** *75* (8), 1036.

(26) Bienstman, P.; Derudder, H; Baets, R.; Olysager, F.; Zutter, D. Analysis of Cylindrical Waveguide Discontinuities Using Vectorial Eigenmodes and Perfectly Matched Layers. *IEEE Trans. Microwave Theory Tech.* **2001,** *49*, 349.

(27) Claudon, J.; Bleuse, J.; Malik, N. S.; Bazin, M.; Jaffrennou, P.; Gregersen, N.; Sauvan, C.; Lalanne, P.; Gerard, J. M. A highly efficient single-photon source based on a quantum dot in a photonic nanowire. *Nat. Photonics* **2010,** *4*, 174.

(28) Friedler, I.; Sauvan, C.; Hugonin, J. P.; Lalanne, P.; Claudon, J.; Gerard, J. M. Solid-state single photon source: the nanowire antenna. *Opt. Express* **2009,** *17* (4), 2095.

(29) Snyder, A. W.; Love, J. D. *Optical Waveguide Theory*; Chapman and Hall: New York, 1983; Chapter 14.